Fast and robust framework for PET-MR attenuation map generation with joint MR bias estimation and tissue segmentation

Dattesh D Shanbhag[1], Sheshadri Thiruvenkadam[1], Sandeep Kaushik[1], Gaspar Delso[2], Scott D Wollenweber[3], Sonal Ambwani[3], Rakesh Mullick[1], and Florian Wiesinger[4]

[1]GE Global Research, Bangalore, Karanataka, India, [2]GE Healthcare, Glattbrugg, Zurich, Switzerland, [3]GE Healthcare, Waukesha, WI, United States, [4]GE Global Research, Garching b. Munchen, Bavaria, Germany

Target Audience: Physicists and Clinicians interested in combined PET-MR imaging and MRI image shading artifact correction

Introduction: In the last few years, significant technical advancements have enabled integrated PET and MR imaging solutions. MR-based PET attenuation correction (AC) is a prerequisite for quantitative PET and a key determining factor for the success of PET/MR. Despite multiple contrasts, MR signal doesn't correlate with PET photon attenuation. Therefore, segmentation based tissue labeling of MR fat-water Dixon images (using e.g. thresholding, clustering, phase-field based) has been suggested to generate the AC maps [1, 2, 3]. Compared to simple thresholding, the phase-field approach is advantageous in that it provides a closed contour solution and has robust performance in the presence of image noise [4]. Despite its advantages, the phase-field based tissue labeling needs to be "*tuned*" to account for spatially-varying RF shading due to B_1 transmit and receive coil sensitivity variations across the body. While RF shading can to a good approximation be neglected with body coil transmit and receive data acquisition [2] it causes the phase-field based segmentation to fail when using phased array coils. However, the latter is advantages from a signal acquisition perspective by providing higher SNR and encoding efficiency using parallel imaging generally resulting in better coverage – resolution – scan time tradeoff. In this work we present a novel approach for MR-AC map generation within the phase field based framework based on joint estimation/correction of the RF shading and tissue label maps using Dixon MRI images; thereby obviating the need to "re-tune" the algorithm for specific cohort of data acquisition. To the best of our knowledge, the presented work describes a novel framework for fast 3D whole body MRI tissue labeling for MRAC purpose.

Methods and Materials: **Simulations:** We initially simulated the framework using synthetic images with super-imposed smooth image shading and with Gaussian distributed noise. **MRI:** Clinical data for our study was obtained using a 3T GE Discovery MR750 scanner in combination with GEM array coils (GE Healthcare, Waukesha, WI). **Patient database:** The database for our study consisted of 5 patients. Multi-station, whole-body MR imaging was performed using a dual-echo spoiled gradient echo sequence (LAVA-Flex) with TR=4ms, FA=12°, TE_1=1.17ms, TE_2=2.39ms, FOV=500x500x258.4mm^3, matrix=256x192x136pts, and 136 slices of 3.8mm thickness and 1.9mm spacing, resulting in 5-7 bed positions for head to pelvic floor coverage. From the obtained MR in-phase (I_{in}) and out-phase images (I_{op}), water (I_w) and fat (I_f) images were reconstructed using DIXON/IDEAL processing. **Joint coil bias estimation and segmentation** (**JBS**): **(a). Bias Map Estimate:** As described in [5,6,7], we assumed a multiplicative model for the image shading with B_{bias} being the shading bias map across the imaging FOV (i.e. $I_{in,shaded} = I_{in,true} * B_{bias}$). An initial pre-processed image was obtained as: $I_{prep} = MAX (I_f / I_{in}, I_w / I_{in})$. This image was combined with a weighted sum of its gradient image to ensure reliable segmentation at the image edge boundary. A reference estimate of the B_{bias} was obtained by low-pass filtering of I_{prep} with a Gaussian kernel (GW-LPF), $B_{bias,ref} = I_{prep} \otimes G_\sigma$ (σ = 5 pixels) [6]. The reference estimate could also be a calibration map as

Seeks Intensity close to c_{air} in region $u = 0$ Seeks Intensity different from c_{air} in region $u = 1$

$$E[u, B_{bias}] = \int_\Omega (1-u)^2 \left(\frac{I}{B_{bias}+\varepsilon} - c_{air}\right)^2 dx + \int_\Omega u^2 \frac{\alpha}{1+\beta\left(\frac{I}{B_{bias}+\varepsilon} - c_{air}\right)^2} dx$$
$$+ \tilde{\lambda}\int_\Omega u^2(1-u)^2 dx + \lambda\int_\Omega |\nabla u|^2 dx + \lambda_{bias}\int_\Omega |\nabla B_{bias}|^2 dx + \tilde{\lambda}_{bias}\int_\Omega (B_{bias}-B_{bias,ref})^2 dx \quad \textbf{Eq. (1)}$$

Constrains u to be {0,1}   Smoothing term for u   Smoothing term for b   Close to ref. bias map

obtained from parallel imaging [5, 8]. **(b). Body Contour:** The body contour was then generated for the specific station data using a 2-class phase field formulation [**Eq.(1)**] to segment out the body mask and provide an estimate of the bias map [3, 4]. In **Eq. (1)**, the two-class function is represented by term "u", with u = 0 representing the background and u=1 the body mask. The first 4 terms seek a smooth class function "u" that separates the image domain into two regions, one where the bias corrected intensity is close to c_{air} and the other where the bias corrected intensity differs from c_{air}. The last two terms seek a smooth bias function B_{bias} that is close to a given reference bias B_{ref}. *The last term is critical for avoiding locally optimal solutions while jointly solving for u and B_{bias}.* Parameters α, β, λ relate to noise variance, sensitivity and smoothness respectively and are manually set. $\tilde{\lambda}_{bias}$ is set very low, close to convergence. The Euler Lagrange cost **Eq. (1)**, is a non-linear PDE, which gets solved by minimizing its energy with respect to "u" using a semi-implicit, iterative and multi-resolution gradient descent framework. **(c). Phase field without bias:** In addition, we also performed segmentation without the bias field term being present (as described in [2]) and using various value of parameter β to get closest matching body mask to in-phase data, as assessed visually. **(d). Lung Segmentation:** The formulation for lung segmentation is similar to Eq.[1] with following changes: *1.* No bias field is estimated, *2.* Intensity corrected image ($I_{corrected}= I_{prep} / B_{bias}$) is used, *3.* The indicator function is reversed so that u = 0 represents the tissue and u = 1 represents the lungs and *4.* Different set of parameters α, β, λ are used. The initial contour for lung segmentation is the body mask. The entire work was implemented in Insight Toolkit (ITK) [9].

Result & Discussion: The joint bias segmentation was found to provide reliable segmentation of the synthetic images, even in presence of significant background noise and recover the signal loss in shaded areas (Fig.1). JBS methodology provides excellent recovery of tissue in the presence of significant RF shading artifacts with phased array coil receive (Fig. 2). The bright areas around the edge of intensity corrected images (Fig 1c, Fig 2c) are primarily due to broad cut-off band of GW-LPF and can be mitigated by using Hamming or Fermi kernels [5]. Moreover, in cases of severe RF shading with the signal intensity similar to that of image background, JBS will not be able to resolve the tissue from the RF shading due to the nature of initial bias map estimate. This was observed in one patient data for distal slices. Notice the accentuation of the background artifacts due to breathing and reconstruction, primarily due to use of input image to generate the initial bias map. However, this can be easily mitigated by providing calibration data from low-frequency k-space data as initial estimate of the bias map or other bias estimation methods [5,7]. The highlighted artifacts don't affect the segmentation of the body mask; primarily due to 3D, multi-resolution (lowest resolution to highest resolution), gradient-weighted approach adopted. As shown in Fig. 3, without JBS, the standard phase-field segmentation approach [2] as used with body coil data results in severe under-segmentation of the body contour. This was found to be resolved by trial and error approach using different values of β parameter, but the lung segmentation leaked into normal tissue due to RF shading. The use of JBS resulted in reliable segmentation of both the body contour and lungs using the default set of parameters [Fig. 3]. Joint segmentation and bias estimation based methods have been previously reported within level set methods [10]. Compared to the approach [10] which works with an energy similar to Multi-phase Chan-Vese (MPCV) framework [11], we incorporate bias correction within a region-growing type formulation using phase-fields (Eq.1). PET-MR system requires robust tissue classification over whole-body data in reasonable time for PET processing. The proposed formulation is much faster for 3D whole body tissue segmentation compared to multi-class formulations as in MPCV and lends itself to key requirement of PET-MR systems. The method also obviates the need for separate, independent intensity correction of the MRI data before tissue segmentation; thereby simplifying the PET-MR workflow as well.

Conclusion: We have successfully demonstrated a novel method for joint MRI RF shading correction and reliable tissue segmentation in context of PET-MR attenuation correction. The method provides for parameter variation resilient body contour and tissue class segmentation across MRI data obtained from different coils and results in simplified workflow for PET-MR attenuation map generation.
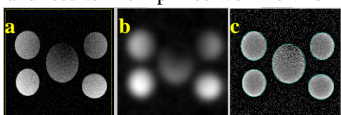

Figure 1. Synthetic images show excellent segmentation (cyan) (c) in presence of noise (a) and (b) shading across image using JBS method

Figure 2. Phased array coil data shows shading across the image (a). The bias map estimated by the JBS methodology (b) and the intensity corrected image is shown in (c). The data is scaled from 0 to 1 for all images
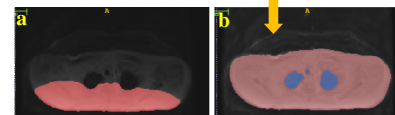

Figure 3. (a). Lack of JBS resulted in severe under-segmentation (b). JBS provides correct body mask (red) and lung (blue) segmentation with same parameters, even in presence of background artifacts [yellow arrow]].

References: *[1]. Martinez-Möller et.al. J Nucl Med 2009 , [2]. Shanbhag et.al. 20th ISMRM 2012, p.4371 [3]. Keereman V et.al., Med. Phys. 38 (11), 2011 [4]. Thiruvenkadam et.al. ICIP 2006 [5]. Murakami et.al. , MRM 35:585-590, 1996 [6]. Wang et.al, MRM: 53:666–674 (2005) [7]. IEEE Trans. Med Img: 26(3), 2007 [8]. Noterdaeme et.al., ISBI 2008: 1525-1528 [9]. www.itk.org [10]. Li C, et. al., LNCS 5242, pp. 1083–1091, 2008 [11]. Vese, L., Chan, T., Int'l. J. Comp. Vis. 50, 271–293 (2002)*